Eur Biophys J (2009) 38:209–218
DOI 10.1007/s00249-008-0371-3

ORIGINAL PAPER

Proteolysis of prion protein by cathepsin S generates a soluble β-structured intermediate oligomeric form, with potential implications for neurotoxic mechanisms

Oxana Polyakova · Denise Dear · Igor Stern · Stephen Martin · Elizabeth Hirst · Suleman Bawumia · Angus Nash · Guy Dodson · Igor Bronstein · Peter M. Bayley

Received: 22 July 2008 / Revised: 9 September 2008 / Accepted: 10 September 2008 / Published online: 24 September 2008

Abstract Formation of PrP aggregates is considered to be a characteristic event in the pathogenesis of TSE diseases, accompanied by brain inflammation and neurodegeneration. Factors identified as contributing to aggregate formation are of interest as potential therapeutic targets. We report that in vitro proteolysis of ovine $PrP_{94–233}$ (at neutral pH and in the absence of denaturants) by the protease cathepsin S, a cellular enzyme that also shows enhanced expression in pathogenic conditions, occurs selectively in the region 135–156. This results in an unusually efficient, concentration-dependent conformational conversion of a large subfragment of $PrP_{94–233}$ into a soluble β-structured oligomeric intermediate species, that readily forms a thioflavin-T-positive aggregate. N-terminal sequencing of the proteolysis fragments shows the aggregating species have marked sequence similarities to truncated PrP variants known to confer unusually severe pathogenicity when transgenically expressed in $PrP^{o/o}$ mice. Circular dichroism analysis shows that PrP fragments 138–233, 144–233 and 156–233 are significantly less stable than $PrP_{94–233}$. This implies an important structural contribution of the β1 sequence within the globular domain of PrP. We propose that the removal or detachment of the β1 sequence enhances β-oligomer formation from the globular domain, leading to aggregation. The cellular implications are that specific proteases may have an important role in the generation of membrane-bound, potentially toxic, β-oligomeric PrP species in pre-amyloid states of prion diseases. Such species may induce cell death by lysis, and also contribute to the transport of PrP to neuronal targets with subsequent amplification of pathogenic effects.

Keywords Proteolysis · Circular dichroism · Thioflavin-T · Truncation mutants · Pathogenicity

Abbreviations

PrP	Prion protein
$PrP_{94–233}$	The globular domain of PrP
PrP^{c}	Cellular PrP
PrP^{Sc}	The scrapie form of PrP
PrP	Proteolytic fragments are identified by their N-terminal sequences, eg 135SAMS
TSE	Transmissible spongiform encephalopathy
ThT	Thioflavin-T
PK	Proteinase K
GuHCl	Guanidine hydrochloride

Electronic supplementary material The online version of this article (doi:10.1007/s00249-008-0371-3) contains supplementary material, which is available to authorized users.

O. Polyakova · S. Martin · E. Hirst · S. Bawumia · A. Nash · G. Dodson · I. Bronstein · P. M. Bayley
National Institute for Medical Research,
Mill Hill, London NW7 1AA, UK

D. Dear · I. Stern
Institute of Biotechnology, University of Cambridge,
Tennis Court Road, Cambridge CB2 1QT, UK

P. M. Bayley (✉)
Division of Physical Biochemistry,
N.I.M.R., London NW7 1AA, UK
e-mail: pbayley@nimr.mrc.ac.uk

Present Address:
I. Bronstein
Department of Biochemistry,
Wolfson Centre for Age-related Diseases,
King's College, London SE1 1UL, UK

Introduction

The prion protein (PrP) is a key molecule in transmissible spongiform encephalopathies or prion diseases, (reviewed in Prusiner 1998). However, the precise mechanism of the transformation in vivo of the normal α-helical containing cellular form (PrP^c) to a highly associated β-structured form, identified by FTIR (Pan et al. 1993), and typified in many diseased states by characteristic deposits, such as the toxic scrapie form, PrP^{Sc}, is still unknown (Caughey and Baron 2006). Extensive biophysical work has demonstrated the conformational conversion of recombinant PrP from α- to β-forms under a variety of in vitro solution conditions that include low pH, denaturants, salts and detergents, often with prolonged mechanical agitation. These treatments result in the formation of β-oligomers and in some cases, amyloid fibril structures. (e.g: Swietnicki et al. 2000; Morillas et al. 2001; Baskakov et al. 2001; Baskakov et al. 2002; Rezaei et al. 2005). Aggregated fibrillar forms of recombinant PrP ('synthetic prions' Legname et al. 2004)) have been shown to cause disease in animal models; however, the demonstration of the toxicity of oligomeric forms of PrP derived from PrP^{Sc} (Silveira et al. 2005) indicates that certain non-amyloidal forms are also potentially toxic.

Many prion diseases associated with natural and transgenically expressed PrP mutants involve a very slow development (Prusiner 1998). By contrast, it has been shown that the expression in transgenic $PrP^{o/o}$ mice of PrP^c containing deletions of amino acids 32–134, 94–134 or 105–125 creates unexpectedly severe neuropathological phenotypes. These include ataxial behaviour and myelin vacuolar degeneration of the brain, occurring without detectable deposition of the typical protease-resistant PrP^{Sc} deposits characteristic of the scrapie condition, (Shmerling et al. 1998; Baumann et al. 2007; Li et al. 2007). The molecular basis of this neuropathology, and its suppression by co-expression of normal PrP^c, is also unknown.

These results indicate a potential role for proteolysed forms of PrP in certain prion disease mechanisms. Intra- and extracellular proteases have been shown to be of potential importance in the modification of neuronal receptors (Saito and Bunnett 2005) and development of prion diseases(Parkin et al. 2007; Yadavalli et al. 2004), and abnormal trafficking, folding and targeting of the cellular protein have been implicated in prion pathogenesis (Tatzelt and Schatzl 2007).

In this work we examine the conformational consequences of proteolysis of PrP by members of a ubiquitous family of proteases, the cathepsins, which exhibit wide-ranging cellular functions [Turk et al. 2000]. Cathepsin S is a cysteine protease that is able to work outside the lysosome and in a wide range of pH; it is secreted by microglia and over-expressed in scrapie brain (Baker et al. 1999; Xiang et al. 2004). We examine the effects of in vitro proteolysis of PrP by cathepsin S, and show that it causes specific and limited N-terminal truncation of $PrP_{94–233}$. This induces an unusually efficient, protein concentration dependent, $\alpha \rightarrow \beta$ conformational conversion, initially forming a soluble β-structured intermediate species, that leads to thioflavin T-positive PrP aggregated species. Sequence analysis of the proteolytic fragments shows a striking similarity between these truncated species and the PrP variants of known high toxicity in $PrP^{o/o}$ transgenic mice, (Shmerling et al. 1998; Baumann et al. 2007; Li et al. 2007). Recombinant expression of the proteolytic fragments shows that the absence of sequences including the β1 residues results in decreased stability and solubility of the PrP globular domain. This suggests proteases may act as a general trigger mechanism for the formation of β-structured oligomeric forms under physiological conditions, and indicates a potential role of proteolytic processes in contributing to rapid toxicity and to longer-term prion pathogenesis.

Experimental

Protein expression and purification

The hexa-His tagged ovine $PrP_{94–233}$ (ARQ allele) was expressed and purified as described (Haire et al. 2004) with small modifications. The cell lysate was centrifuged at 20,000*g* for 20 min. The resulting pellet was dissolved in buffer A (10 ml per 1 g of pellet; 100 mM Tris (pH 8.0), 8 M Urea), incubated for 2 h at room temperature, and centrifuged at 20,000*g* for 15 min to remove insoluble material. The solubilized inclusion bodies were incubated with Ni-NTA Agarose (Qiagen) at 4°C for 1 h on a rocker table. The NTA column was washed to remove unbound protein with five volumes of buffer A. Refolding of PrP was achieved with PrP still bound to the resin by resuspending the pelleted resin in cold refolding buffer (50 mM Tris, pH7.5). This mixture was incubated for 30 min at 4°C with rocking. PrP was eluted from the resin in refolding buffer supplemented with 500 mM imidazole pH 7.5, and dialyzed against 50 mM sodium acetate (pH 5.5). The purity of the final rPrP preparation was confirmed by SDS-PAGE, and far UVCD spectroscopy was used to confirm the correctly folded structure. Protein concentration was determined on the Jasco V550 spectrophotometer, with a calculated ε_{280} for $OvPrP_{94–233}$ of 23,505 M^{-1} cm^{-1}. $OvPrP_{138–233}$, $PrP_{144–233}$ and $PrP_{156–233}$, were similarly expressed, but with a protease-sensitive His tag that is removed either in the NTA-attached state, or following the imidazole elution step. Prolonged storage of PrP in Tris buffer was avoided, since it causes degradation.

Circular dichroism spectroscopy and analysis

CD experiments were performed at 30°C in 50 mM MES at pH 5.5–6.5 with protein concentrations 6–60 μM in a 1 or

0.2 mm (demountable) cuvette. CD spectra were recorded from 260 to (maximally) 190 nm on a Jasco J-715 spectropolarimeter at 20 nm/min with bandwidth 2.0 nm. 25 CD scans were averaged, smoothed by instrumental software and the data expressed as CD extinction coefficient, $\Delta\varepsilon_{mrw}$ ($M^{-1}\,cm^{-1}$). CD spectra were analysed by the method of CONTIN, (Provencher and Glockner 1981), using the set of spectra of 48 proteins, SD48, that includes five denatured proteins, (Sreerama and Woody 2000). Data were smoothed with standard polynomial procedures; truncation of data to 205 nm did not significantly affect the numerical analysis results. In all cases the curve fitting was within the experimental noise level of the accumulated spectrum. The numerical results for composition in terms of α-helix, β-sheet, turns and aperiodic (coil) structure were fully consistent with those from analysis by alternative analytical methods. Unfolding studies were performed with heating rate 1°/min, and cooling rate (for $PrP_{94–233}$) 2°/min.

Digestion of PrP by cathepsin S and other proteolytic enzymes

The $PrP_{94–233}$ (20–60 μM) was treated with cathepsins S L or D at 30°C at different weight ratios of prion protein to enzyme in aqueous buffer at pH 5.5–7.5, containing 0.2 mM DTT and 0.2 mM EDTA. The digestion was carried out in 100 μl volume in 96-well plates (Safire 2, TECAN) in the presence of 100 μM ThT, (Breydo et al. 2005). The plate was sealed with ImmunoWare tape. The kinetics were monitored by bottom reading of fluorescence intensity every 10–15 min using monochromator settings of 444 nm excitation and 485 nm emission and 5 nm bandpass, which were shown to ensure fluorescence was monitored with full exclusion of possible light scattering artefacts. Digestion of $PrP_{94–233}$ by calpain-1 was performed in aqueous buffer, pH 5.5 containing 1 mM Ca^{2+} and 0.2 mM DTT. Stock solutions were diluted as indicated. All proteases were from Merck.

Mass spectrometric analysis

ESI-MS (electrospray ionization mass spectrometry) was used to analyze the soluble products of PrP after 10 min digestion of PrP (160 μM) with cathepsin S (0.1 μM) at room temperature in 50 mM sodium acetate (pH5.5).

N-terminal protein sequence analysis and Western blot

$PrP_{94–233}$ (100–160 μM) was digested by cathepsin S (0.06–0.1 μM) under standard conditions in Eppendorf tubes. The proteolytic products were analyzed during the time course over a period of 24 h. For N-terminal sequencing, aliquots of the digestion mixture were heated at 95°C for 15 min and analyzed by SDS-PAGE (4–12% NuPage Mes system : Invitrogen) under non-reducing conditions, and blotted onto Immobilon PSQ PVDF membrane (Millipore). N-terminal sequencing was performed by the PNAC Facility, (University of Cambridge). For Western blot experiments, protein bands were electro-blotted onto the membrane, incubated with anti-PrP mAb AH6 (1 μg/ml) (IAH, Compton, UK) followed by incubation with donkey anti-mouse IRQye800 conjugate (1:5,000 dilution, Rockland) and fluorescent detection on Odyssey® Imaging System (Li-Cor Biotechnology).

Proteinase K digestion

The pelleted material after digestion of $PrP_{94–233}$ (0.5 mg/ml) by cathepsin S was treated with Proteinase K (Qiagen) in 50 mM Tris (pH 7.5) at 37°C, using different weight ratios of PrP to PK. Aliquots were removed over a period of 48 h and digestion was stopped by quenching with 2 mM PMSF plus 4 × SDS sample buffer, with SDS-PAGE analysis as above.

Results

Plate reader fluorescence assay of PrP aggregation

The time course of digestion of $PrP_{94–233}$ by cathepsin S, (studied in a 96-well plate format (Breydo et al. 2005), showed a progressive increase in ThT fluorescence with a characteristic lag phase and eventual attainment of a plateau, correlating with production of aggregated material. Figure 1a–d shows that increased concentrations of either cathepsin S or PrP diminishes the lag phase and increases the plateau value. Similar behaviour is seen from pH 5.5 to 7.5. This corresponds to the pH range encountered in normal plasma conditions as well as the internal pH of vesicles. At the higher pH values, and with increased concentration of cathepsin S, the plateau eventually decreases, correlating with the digestion of the aggregated material.

Analysis of proteolytic fragments

The time-dependent evolution of the products of the digestion of $PrP_{94–233}$ by cathepsin S at ratio 1:1,500, was analysed on non-reducing SDS PAGE gels for the total digestion mixture, Fig. 2a and for the precipitate and supernatant separated by centrifugation, (Fig. 2b, c). The precipitate and supernatant account for all the bands observed in the total digest. No precipitate was observed at time zero, but became evident at approximately 3 h, increasing thereafter, Fig. 2b. Soluble PrP fragments are identified from

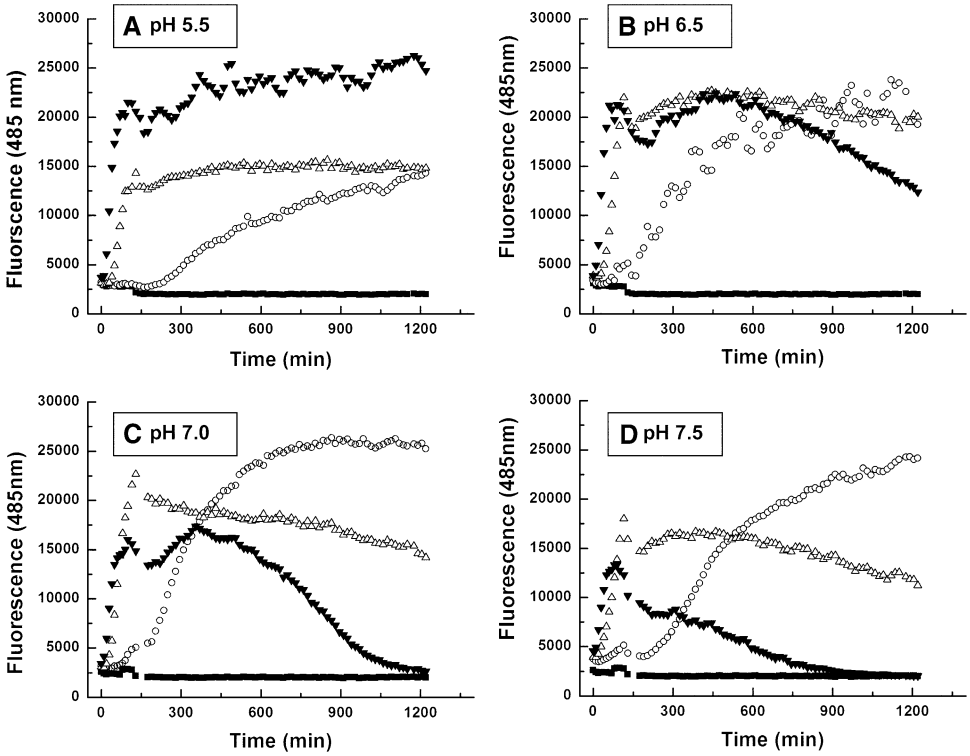

Fig. 1 The ThT-binding assay kinetics digestion of 20 μM $PrP_{94–233}$ by cathepsin S at 30°C, at pH values 5.5–7.5 (**a**–**d**), and at different ratios of $PrP_{94–233}$ to cathepsin S,(*open circle*) 1500:1, (*open triangle*) 200:1, (*inverted filled triangle*) 50:1. Control: (*filled square*) undigested $rPrP_{94–233}$

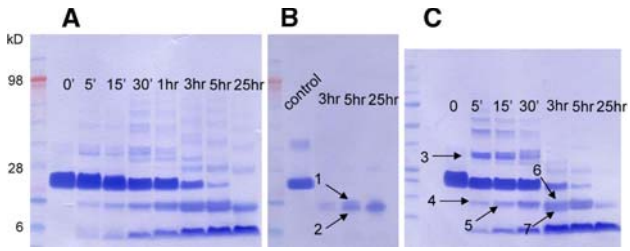

Fig. 2 PAGE analysis of the time course of digestion of 60 μM $PrP_{94–233}$ by 0.04 μM cathepsin S (1,500:1) at 30°C, pH5.5. **a** Total digestion mixture; **b** precipitate; **c** supernatant. Control: PrP incubated alone (3 h) in digestion buffer containing 0.2 mM DTT. The numbered bands were subjected to N-terminal sequence analysis

t = 30 min onwards in bands 3,4,5,6 and 7, Fig. 2c. The gels were blotted for N-terminal sequencing of the numbered bands, and the relative amounts of the different proteolytic fragments are presented in Table 1. N-terminal analysis shows that the precipitate (band 1–2, Fig. 2b) is composed of fragments with N-terminal sequences 135SAMS and 144FGND in similar quantities. Fragments in the supernatant (bands 4–7) correspond to 135SAMS and shorter sequences, and the fastest band which contains the N-terminal His tag sequence of the recombinant $PrP_{94–233}$.

An initial mass spectrometry analysis of the digestion mixture identified three major soluble fragments $PrP_{135–233}$, $PrP_{117–233}$, and $PrP_{114–233}$, (data not shown). Also, on reducing gels, all bands (except band 3, which was absent) behaved identically. These two results indicate that no proteolytic cleavage of $PrP_{94–233}$ has occurred between Cys_{182} and the C-terminus, Ala_{233}, (since this would have led to a band of lower mass on the reducing gel) and aggregation does not involve intermolecular disulphide exchange (since pronounced differences would have been observed with the non-reducing gel). The soluble band 3 also contains the His tag, and is apparently a disulphide linked PrP species, attributable to the presence of 0.2 mM DTT required to maintain cathepsin activity. It is also seen as a minor species in the absence of cathepsin S, (control, Fig. 2b). At higher ratios of cathepsin S, the 144FGND fragment constitutes a larger proportion of the insoluble precipitate, approaching equivalence with 135SAMS. Thus the presence of 144FGND in the digest correlates with the appearance of aggregation.

Cleavage patterns of PrP with other proteases

N-terminal sequence analysis of these bands was used to identify the cleavage patterns of PrP with several cathepsins and calpain-1, which are summarized in Fig. 3. Of these enzymes, cathepsin B and calpain-1 yield soluble fragments whereas cathepsins S and L are most effective in producing ThT-positive aggregates. Cathepsin S shows major cleavage sites at 135SAMS and 144FGND, associated with aggregation. Cathepsin L has three main cleavage sites and produces a precipitate with 135SAMS, 144FGND and 146NDYE in similar amounts, together with significant amounts of shorter species 160YPNQV

Table 1 Approximate relative amounts of different fragments produced by digestion of $PrP_{94–233}$ by cathepsin S, determined by N-terminal sequence analysis

	Sequence	GHH	HVA	GAA	GLG	GYM	135SAM	DYE	144FGN
Band	Pmoles		%	%	%	%	%	%	%
PPT:1							Positive		Trace
PPT:2							Positive		Positive
SUP:3		Positive							
SUP:4	50		56	40	4				
SUP:5	28		21	21	29	7	21		
SUP:6	177		48	46	4		3		
SUP:7	106		14	33	19		28	5	

Relative amounts of material analysed in bands 1–2 (precipitate, from Fig. 2b) and for bands 3–7 (supernatant Fig. 2c), the total amount (pmoles), and the percentage of a given fragment. Fragments are denoted by the initial sequence of three residues. The GHH fragment represents a sequence with the intact N-terminal tag, apparently a dimeric PrP species in the minor band 3 of the supernatant. The control (Fig. 2) shows a minor contamination of this species in the absence of digestion, probably due to the low concentration of DTT present in the buffer in order to maintain the protease activity

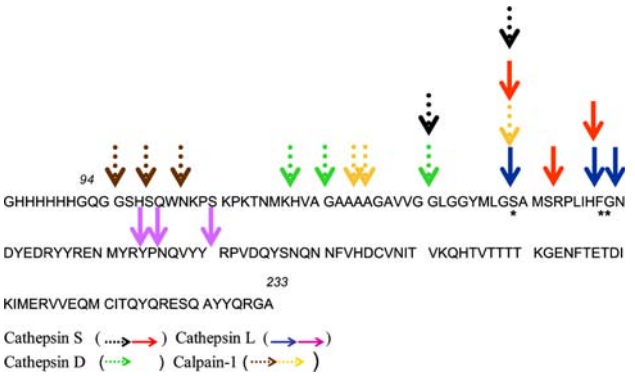

Fig. 3 Summary of N-terminal sequencing data for digestion of $PrP_{94–233}$ by different cathepsins. *Dotted arrows* indicate the N-terminus of cleavage products that do not generate the precipitate; *solid arrows* indicate products which form precipitate. Residues 135 and 144 are denoted *single asterisk* and *double asterisks*

and 167RPVDQ. Calpain-1 shows major cleavage sites at 120AAGA and 135SAMS, but does not lead to aggregate formation on the same time scale as cathepsin S. Hence cleavage beyond 135SAMS appears to increase the yield of aggregates.

Properties of the aggregated material

A major characteristic of PrP^{Sc}, the disease-associated, aggregated form of PrP, is its increased resistance of the protein to digestion by the bacterial proteinase K (PK). Compared with amyloid fibrils prepared in vitro (Baskakov et al. 2002), the resistance of the pelleted material from the cathepsin S digestion was significantly reduced (data not shsown). Optical and electron microscopy of the products identified in the ThT assay showed mainly the presence of associations of approximately spherical aggregates, rather than amyloid fibrils (see Supplementary Material, Figure S1).

Structural changes of PrP during cathepsin S proteolysis

Monitoring the time course of the digestion process continuously by far UV circular dichroism shows that the conformational consequences are dependent on the protein concentration. Figure 4a, with (PrP) = 9 μM, shows the progressive and extensive loss of the typical α-helical content of $PrP_{94–233}$, ($\alpha = 38\%$, $\beta = 14\%$, turn = 19%, coil = 29%) with conversion to a largely random coil form

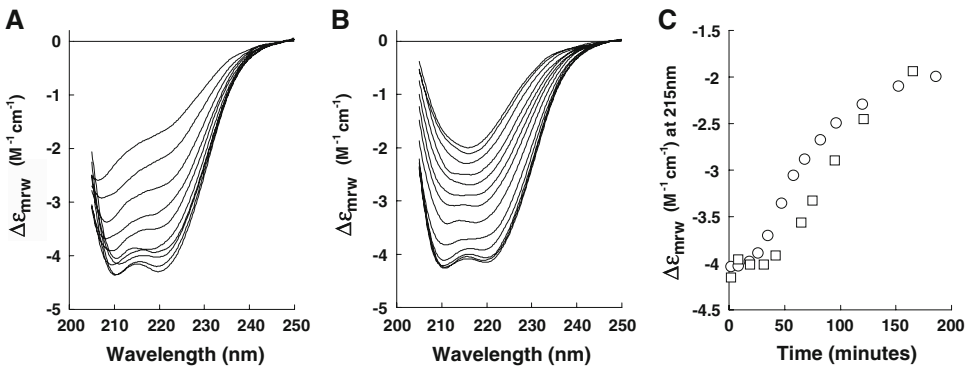

Fig. 4 Time course of the decrease in far UV circular dichroism showing the conformational change of $PrP_{94–233}$ digested by cathepsin S (200:1 w/w) in Mes 50 mM pH 6.5, at 30°C; **a** 9 μM PrP and **b** 60 μM PrP; **c** $\Delta\varepsilon_{mrw}$ at 215 nm as function of time for 9 μM (*open square*), 60 μM (*open circle*)

($\alpha = 11\%$, $\beta = 13\%$, turn = 17%, coil = 59%). By contrast, with (PrP) = 60 μM, there is a progressive conversion of the spectrum of the α-helical form to one with a single negative trough at 215 nm, typical of β-structured species, Fig. 4b. Analysis shows the final conformation ($\alpha = 9\%$, $\beta = 33\%$, turn = 24%, coil = 34%), indicating a substantial loss of α-helix and a predominantly $\alpha \rightarrow \beta$ conformational transition. During the digestion period, under both conditions, there was no evidence of CD signal distortion above 195 nm from light scattering, and no turbidity was detectable by visual inspection. The spectrometer dynode voltage remained constant at 364.3 ± 1.1 for A, and 374.2 ± 1.2 for B, indicating the constancy of the optical transmission of the samples. This demonstrates that in both cases, the initial digestion product did not precipitate under the conditions of the CD experiments. The concentration dependence of this $\alpha \rightarrow \beta$ transition indicates that molecular association occurs at the higher concentration, with formation of a soluble β-structured intermediate that precedes the aggregation process. The time course of the CD changes are similar in both cases (Fig. 4c) with the presence of a lag phase indicating that the conformational effects are dependent on the initial proteolysis, and that the oligomeric molecular association at the higher concentration is relatively rapid. Control experiments of $PrP_{94–233}$ digested with calpain-1 show a slower decrease of α-helix and gain of both β and (turn + coil) conformational components (data not shown). However, in contrast to the cathepsin S experiments, no aggregation was observable in digestion with calpain-1 in the plate assay even after several days incubation.

Stability studies

In order to further characterize the conformational differences between $Prp_{94–233}$ and its N-terminal truncations, the sequences $PrP_{138–233}$, $PrP_{144–233}$ and $PrP_{156–233}$ were expressed and purified, and their thermal stability compared to that of $PrP_{94–233}$ was examined by far UV circular dichroism. All showed decreased solubility and a tendency to slow aggregation in Tris pH 7.5, buffer, but, at low concentration, all species showed a single thermal unfolding transition, Fig. 5a. This was only partially reversible on cooling, (~50% for $PrP_{94–233}$ and 20% for the shorter fragments), with visible turbidity. All fragments were significantly more soluble in 1 M GuHCl, without significant loss of normal α-helical secondary structure. Effectively fully (>95%) reversible thermal unfolding was observed $PrP_{94–233}$ in 1 M GuHCl with a $T_m = 58.2$°C. Reversibility of 90, 85 and 75, and T_m values of 48.3, 47.1 and 45.6°C were observed for $PrP_{138–233}$, $PrP_{144–233}$ and $PrP_{156–233}$, respectively, Fig. 5b. These results indicate a significant discontinuous loss of thermodynamic stability of these species lacking N-terminal residues preceding α-helix 1. This sequence includes the short β1 seqeunce (MLG,132–134) that engages in antiparallel, intramolecular interaction with β2, (QVY,163–165). The near UV CD of $PrP_{94–233}$ shows that the conformation of aromatic side-chains is significantly affected by the presence of 1 M GuHCl, Fig. 5c. (Ov)$PrP_{94–233}$ contains a single Trp residue (W102) in a region that appears unstructured in both NMR and crystallographic studies (Haire et al. 2004), plus 12 Tyr residues, which are located in two clusters within the globular domain linked by helix 3, and which include three Tyr–Tyr dipeptide repeats. The difference spectrum (Fig. 5c) has the form of a CD 'couplet', with positive and negative lobes, consistent with electronic interactions amongst the Tyr residues being at least partially disrupted in 1 M GuHCl. The perturbation of tertiary structure with unchanged secondary structure is typical of a molten globule conformation. This state has recently been proposed for the β-rich oligomeric form of PrP (O'Sullivan et al. 2007), and for an intermediate conformational precursor (Gerber et al. 2007), both observed under mildly denaturing and low pH conditions in vitro.

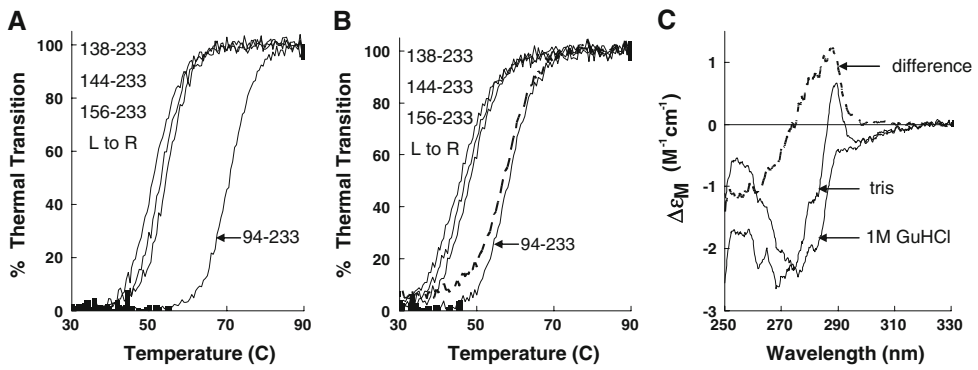

Fig. 5 Stability studies: **a** and **b** thermal unfolding of $PrP_{94–233}$, $PrP_{138–233}$, $PrP_{144–233}$ and $PrP_{156–233}$ in **a** 50 mM Tris buffer, pH 7.5 and **b** the same containing 1 M GuHCl: the *dashed line* is the cooling curve for $PrP_{94–233}$. In all cases, the unfolding transition represents a decrease of 27–40% of the signal at 215 nm. **c** Near UVCD of $PrP_{94–233}$ in Tris, and Tris plus 1 M GuHCl; (*dashed line*) the difference spectrum

Interestingly, the use of 1 M GuHCl has been the basis of several in vitro conformational conversion assays for PrP (Caughey et al. 1999), and partially denaturing conditions involving low pH, GuHCl, urea and salt, plus mechanical agitation) are well established means of generating Prp amyloid fibrils (Morillas et al. 2001; Baskakov et al. 2002). We conclude that loss of the β-1 sequence by proteolysis under more normal neutral solution conditions causes a significant conformational perturbation of the globular domain of Prp, leading to α–β transformation, accompanied by oligomerisation of the β state.

Discussion

Previous extensive studies have illustrated the ability of several unstructured peptide fragments of PrP to adopt β-structure and to form insoluble fibrils, often at low pH, mimicking the conditions of the endosomal compartment, (Tagliavini et al. 2001; Jamin et al. 2002). In fact the short sequence $PrP_{172–178}$ is closely related to the Sup35 heptapeptide that has been shown to form a β-structured polar zipper, (Nelson et al. 2005; Sawaya et al. 2007). In addition, the mixtures of digestion products of PrP with common non-physiological proteases have been shown by dynamic light scattering to produce large aggregates in a time-dependent process, (Georgieva et al. 2004). No correlation has been established to date between such short fragments and potential pathogenicity in prion diseases. However these results indicate a number of possible candidates for initiation of β-structure formation in PrP, or alternatively that, once initiated, β-structure can become the predominant conformation for a large fraction of the sequence, possibly limited by the persistence of the intramolecular disulphide bond.

We show by N-terminal sequence analysis that the region of PrP between S135 and N146 is a major target for selective cleavage cathepsins S and L. The proteolysis by calpain-1 produces mainly 135SAMS, but without aggregation on the same time scale. We deduce that the shorter fragment, 144FGND, apparently formed from, or in parallel with, 135SAMS by cathepsin S, is an efficient promoter of this aggregation step. Monitoring of the cathepsin S-dependent assembly process by ThT fluorescence and of protein conformation by far-UV CD indicates the initial formation of a soluble form of proteolysed PrP species that loses much of the α-helical structure (initially$\sim$38%), and adopts a conformation with a significantly increased proportion ($\sim$33%)of β-structure. The structural mechanism whereby proteolysis leads to this conformational conversion involves cleavage of the globular domain $PrP_{94–233}$ in the region of residue S135, leading to more extensive proteolysis by cathepsin S. In the intact globular domain, (with helices 2 and 3 linked by the disulphide bridge), the helices 1–3 form the stable core of the globular domain with the lowest degree of thermal motion (Haire et al. 2004), β1 and β2 strands form the short β-sheet, and residues 134 to 137 are relatively mobile. The thermal stability studies show that sequences lacking the β1 strand are significantly less stable than $PrP_{94–233}$, and are more prone to aggregation. In the absence of β1, the detachment of the relatively mobile extended sequence (135–144) prior to α-helix H1 could give access to the cathepsin-specific site prior at 144F, and the proteolytic release of residues up to 144F exposes several hydrophobic residues. The formation of the 144FGND fragment by cathepsin S promotes the formation of the strongly ThT-positive aggregated form containing both 135SAMS and 144FGND. The far UVCD data indicate that the species initially formed with enhanced intermolecular β-structure are soluble and hence are conformational precursors of the aggregated state.

The destabilisation of the core of the globular domain by proteolysis in the region between the secondary structural elements β1 and α-helix H1 is consistent with previous conformational studies on two N-terminal deletion/truncation mutants of mouse PrP globular domain 121–231, mutant ΔH1 with H1 replaced by a short β-turn, and mutant H2H3, $MoPrP_{170–231}$, that lacks β1, but contains the two last helices, (Eberl and Glockshuber 2002). Both mutants are significantly destabilized relative to the globular domain ($MoPrP_{121–231}$). Both retain some α-helical structure, but, consistent with the present findings, mutant H2H3 is the less stable. The extensive conformational conversion on proteolysis of PrP by cathepsin S observed by far UVCD must involve a substantial fraction of the residues of the PrP globular domain, and this conformational conversion is further driven by intermolecular association to produce the soluble oligomeric intermediate.

The key role of the β1 sequence as shown by the proteolysis results suggets a consistent molecular mechanism for the generation of extensive β-sheet structure of PrP under different conditions. Denaturants and detergenets at concentrations less than those required to cause equilibrium unfolding of the globular domain could also affect the stability of the β1–β2 interaction. Low pH could act similarly as shown by molecular dynamic simulation (Alonso et al. 2001). The sequence immediately following β1 shows high thermal factors in the crystal structure and mobility in NMR properties (Haire et al. 2004), indicating only weak interaction with the globular domain. Thus in these cases the disruption of the intramolecular β1–β2 sheet by partial denaturation, as with the removal of the β1 sequence by proteolysis, could act as a trigger that initiates the increase of β-structure within the domain, leading to self-association and aggregation of the β-oligomer.

Cellular implications

The early sites for proteolysis of $PrP_{94–233}$ by these cathepsins that result in aggregation occur selectively in the N-terminal region of the globular domain, implying that, in vivo, similarly proteolysed PrP^{c} would retain its GPI anchor and thus would remain attached to the plasma membrane. This suggests the possibility that such a membrane bound proteolytically N-truncated PrP could concentrate locally and self-associate to form β-rich intermediates of PrP under physiological conditions that could act as nuclei for the longer-term formation of higher oligomers. In addition, as reported for the toxicity of oligomers of a number of amyloidogenic sequences, they could themselves act as potent pathogenic lytic agents, (Kayed et al. 2004; Walsh and Selkoe 2007). The CD analysis shows that a key factor in the $\alpha \rightarrow \beta$ conformational conversion of PrP is the local concentration of the destabilised proteolytic fragment. When the fragment is expressed in a $Prp^{o/o}$ mouse, it would presumably be at relatively high local concentration at the plasma membrane, and could be toxic per se, or rendered so by very limited proteolysis and aggregation. In the presence of co-expressed wt-Prp, known to abrogate the rapid neonatal pathogenesis, the local concentration of the fragment would be reduced, and conversion or toxicity would be significantly retarded.

Current knowledge (Silveira et al. 2005; Tatzelt and Schatzl 2007) suggests that prion diseases may reflect a multiplicity of distinct but not necessarily exclusive mechanisms. Theserelect phenomena observed on widely different time-scales. On the one hand, the transmissibility of an 'infectious' form of PrP, is characterized by the progressive but slow appearance of a proteinase K-resistant aggregated form (PrP^{Sc}) containing enhanced β-structure possibly generated in an endosomal low pH environment. Alternatively the involvement of various mutated, truncated and deleted PrP variants can lead to pathogenic phenotypes, that, in view of their potency, act too rapidly to allow accumulation of the PrP^{Sc} species. The striking finding of our work is that cathepsin proteases, normal physiological enzymes that are also associated with pathogenic conditions, readily generate specific fragments of $PrP_{94–233}$ with a clear and striking sequence similarity to deletion and truncation mutants of PrP, modified in the region of sequence β1, that are highly toxic when expressed transgenically, (Baumann et al. 2007; Li et al. 2007). In addition, the efficient formation of β-structured PrP oligomers by proteolysis implies a potential role in the early stages of certain pathogenic conditions. However the existence of numerous disease-related point mutations and associated variants throughout the PrP sequence (Prusiner 1998) indicates that other regions of PrP exert important influences throughout the development of the pathogenic responses. It could be highly informative to assess the relative contributions of these factors using experimentally generated PrP variants with mutations to key residues within the protease sensitive regions to prevent proteolysis.

Extracellular proteases have been implicated in both physiological and pathological states in the central nervous system. Some play a crucial role in neuronal migration, neurite outgrowth and synaptic plasticity. Others are required for neuronal death and tumour growth and invasion. Various insults can disrupt the fine control of proteolysis and cause pathological changes (Zhang et al. 2005). Cathepsin S is able to work outside the lysosome and in a wide range of pH. It is especially expressed in cells of a mononuclear lineage including microglia. Gene knock-out results have revealed that cathepsin S and other cathepsins carry out their specific functions by limited proteolysis of proteins (Turk et al. 2000). There is increasing evidence that disturbance of the normal balance of cathepsins contribute to neurodegeneration (Nakanishi 2003). One of the recently discovered functions of cathepsin S in the brain is its role in the migration and activation of microglia to protect motor neurons against injury, (Hao et al. 2007). It was shown that cathepsin S releases a soluble chemokine FLK from the cellular surface of some neurons that is able to stimulate microglia to secrete specific soluble mediators of neuronal activity (Clark et al. 2007). New data demonstrate that cathepsin S is also involved in some important pathological events including Alzheimer and prion diseases. The activation of cathepsins was found to be an upstream event in the experimental scrapie model (Xiang et al. 2004). The ME7 model of murine prion disease shows an atypical inflammatory response characterized by morphologically activated microglia and an anti-inflammatory cytokine profile with a marked expression of TGF-β1 (Baker et al. 1999). TGF-β1 plays a critical role in the down-regulation of microglial responses minimizing brain inflammation and damage caused by reactive oxygen species and extracellular proteases. Up-regulation of cathepsin S and other cathepsins in activated glia may significantly contribute to neurodegeneration. Cathepsin S was found in exosomes released by activated microglia (Potolicchio et al. 2005). This observation may provide a mechanism of a fast and specific delivery of cathepsin S and other reagents to neurons that could be mediated via exosomes released by activated microglia. The physiological advantage of exosome transport in the brain can be justified because this organ, in which cell motility is greatly restricted, needs an integral reliable communication between glia and neurons to support neuronal metabolism and to act quickly in response to brain injury, proinflammatory events and invasion of pathogens. However, exosomes have also recently been reported to be carriers of proteins associated with several amyloid diseases

including prion disease (Vella et al. 2007), and hence transported PrP could also serve to amplify incipient neuropathogenic conditions. It would clearly be of interest to know if there is link between proteolysis, conversion and aggregation process, and the generation and secretion of exosomes. Elevated levels of PrP^c expression in the presence of reactive oxygen and nitrogen species, rapid recycling, specific proteolysis and significant pH dependent conformational changes suggest that PrP^c is able to sense various external stimuli and to transmit conformational changes into intra- and intercellular signals. The loss of the N-terminus may disrupt normal PrP functions and cause the anomalous signalling of truncated protein (Shmerling et al. 1998). PrP is also very sensitive to other abnormal interactions such as the cross-linking anti-PrP monoclonal antibodies D13 and P that were shown to be highly toxic in in vivo experiments (Solforosi et al. 2004). These data show that there are multiple ways in which PrP may lose its function and might convert into a toxic form, including the loss of the N-terminus as a result of specific proteolytic cleavage.

The in vitro proteolysis studies reported here represent a substantial simplification of the complex physiological system, reduced to the actions and interactions of a small number of purified components. In this case we have concentrated on the action on PrP of cathepsin S, in view of its specific elevation in conditions of scrapie pathogenesis, though the findings would apply to any physiological protease of the requisite specificity. Examination of the potential toxicity of the individual fragments identified in this work remains to be performed. While experiments on PrP conversion in vitro and in vivo generally relate to very different time scales, the observations of severe and relatively rapid pathogenicity by the transgenic expression of deletion and truncation mutants of PrP correlate with sequences that also show slow aggregation appear to bring the two experimental time domains into closer proximity. The ability of coexpressed wt-PrP^c to suppress the pathogenic effects of the mutant proteins might suggest normal cellular disposal mechanisms can provide only limited protection against a low threshold of toxic products. However, these mechanisms may be insufficient to counteract the effects of a localized overload of aggregated material and enhanced protease activity under disease conditions. Understanding of this important protective mechanism would add significantly to the identification of agents highly relevant to the development of therapeutic interventions against prion diseases.

Acknowledgments We thank Stephen Howells, NIMR, for mass spectrometry. This work was supported by Department of Health (UK) via grants 0070106 to PB and 007/015 to IB, and by the Medical Research Council (UK). IS was supported by a travel grant from the Royal Society, London.

References

Alonso DO, DeArmond SJ, Cohen FE, Daggett V (2001) Mapping the early steps in the pH-induced conformational conversion of the prion protein. Proc Natl Acad Sci USA 98:2985–2989. doi:10.1073/pnas.061555898

Baker CA, Lu ZY, Zaitsev I, Manuelidis L (1999) Microglial activation varies in different models of Creutzfeldt–Jakob disease. J Virol 73:5089–5097

Baskakov IV, Legname G, Prusiner SB, Cohen FE (2001) Folding of prion protein to its native alpha-helical conformation is under kinetic control. J Biol Chem 276:19687–19690. doi:10.1074/jbc.C100180200

Baskakov IV, Legname G, Baldwin MA, Prusiner SB, Cohen FE (2002) Pathway complexity of prion protein assembly into amyloid. J Biol Chem 277:21140–21148. doi:10.1074/jbc.M111402200

Baumann F, Tolnay M, Brabeck C, Pahnke J, Kloz U, Niemann HH, Heikenwalder M, Rulicke T, Burkle A, Aguzzi A (2007) Lethal recessive myelin toxicity of prion protein lacking its central domain. EMBO J 26:538–547. doi:10.1038/sj.emboj.7601510

Breydo L, Bocharova OV, Baskakov IV (2005) Semiautomated cell-free conversion of prion protein: applications for high-throughput screening of potential antiprion drugs. Anal Biochem 339:165–173. doi:10.1016/j.ab.2005.01.003

Caughey B, Horiuchi M, Demaimay R, Raymond GJ (1999) Assays of protease-resistant prion protein and its formation. Methods Enzymol 309:122–133. doi:10.1016/S0076-6879(99)09011-4

Caughey B, Baron GS (2006) Prions and their partners in crime. Nature 443:803–810. doi:10.1038/nature05294

Clark AK, Yip PK, Grist J, Gentry C, Staniland AA, Marchand F, Dehvari M, Wotherspoon G, Winter J, Ullah J, Bevan S, Malcangio M (2007) Inhibition of spinal microglial cathepsin S for the reversal of neuropathic pain. Proc Natl Acad Sci USA 104:10655–10660. doi:10.1073/pnas.0610811104

Eberl H, Glockshuber R (2002) Folding and intrinsic stability of deletion variants of PrP(121–231), the folded C-terminal domain of the prion protein. Biophys Chem 96:293–303. doi:10.1016/S0301-4622(02)00015-7

Georgieva D, Koker M, Redecke L, Perbandt M, Clos J, Bredehorst R, Genov N, Betzel C (2004) Oligomerization of the proteolytic products is an intrinsic property of prion proteins. Biochem Biophys Res Commun 323:1278–1286. doi:10.1016/j.bbrc.2004.08.230

Gerber R, Tahiri-Alaoui A, Hore PJ, James W (2007) Oligomerization of the human prion protein proceeds via a molten globule intermediate. J Biol Chem 282:6300–6307. doi:10.1074/jbc.M608926200

Haire LF, Whyte SM, Vasisht N, Gill AC, Verma C, Dodson EJ, Dodson GG, Bayley PM (2004) The crystal structure of the globular domain of sheep prion protein. J Mol Biol 336:1175–1183. doi:10.1016/j.jmb.2003.12.059

Hao HP, Doh-Ura K, Nakanishi H (2007) Impairment of microglial responses to facial nerve axotomy in cathepsin S-deficient mice. J Neurosci Res 85:2196–2206. doi:10.1002/jnr.21357

Jamin N, Coic YM, Landon C, Ovtracht L, Baleux F, Neumann JM, Sanson A (2002) Most of the structural elements of the globular domain of murine prion protein form fibrils with predominant beta-sheet structure. FEBS Lett 529:256–260. doi:10.1016/S0014-5793(02)03353-7

Kayed R, Sokolov Y, Edmonds B, MacIntire TM, Milton SC, Hall JE, Glabe CG (2004) Permeabilization of lipid bilayers is a common conformation-dependent activity of soluble amyloid oligomers in protein Mis-folding diseases. J Biol Chem 279:46363–46366. doi:10.1074/jbc.C400260200

Legname G, Baskakov IV, Nguyen HO, Riesner D, Cohen FE, DeArmond SJ, Prusiner SB (2004) Synthetic mammalian prions. Science 305:673–676. doi:10.1126/science.1100195

Li A, Christensen HM, Stewart LR, Roth KA, Chiesa R, Harris DA (2007) Neonatal lethality in transgenic mice expressing prion protein with a deletion of residues 105–125. EMBO J 26:548–558. doi:10.1038/sj.emboj.7601507

Morillas M, Vanik DL, Surewicz WK (2001) On the mechanism of alpha-helix to beta-sheet transition in the recombinant prion protein. Biochemistry 40:6982–6987. doi:10.1021/bi010232q

Nakanishi H (2003) Neuronal and microglial cathepsins in aging and age-related diseases. Ageing Res Rev 2:367–381. doi:10.1016/S1568-1637(03)00027-8

Nelson R, Sawaya MR, Balbirnie M, Madsen AO, Riekel C, Grothe R, Eisenberg D (2005) Structure of the cross-beta spine of amyloid-like fibrils. Nature 435:773–778. doi:10.1038/nature03680

O'Sullivan DB, Jones CE, Abdelraheim SR, Thompsett AR, Brazier MW, Toms H, Brown DR, Viles JH (2007) NMR characterization of the pH 4 beta-intermediate of the prion protein: the N-terminal half of the protein remains unstructured and retains a high degree of flexibility. Biochem J 401:533–540. doi:10.1042/BJ20060668

Pan KM, Baldwin M, Nguyen J, Gasset M, Serban A, Groth D, Mehlhorn I, Huang Z, Fletterick RJ, Cohen FE et al (1993) Conversion of alpha-helices into beta-sheets features in the formation of the scrapie prion proteins. Proc Natl Acad Sci USA 90:10962–10966. doi:10.1073/pnas.90.23.10962

Parkin ET, Watt NT, Hussain I, Eckman EA, Eckman CB, Manson JC, Baybutt HN, Turner AJ, Hooper NM (2007) Cellular prion protein regulates beta-secretase cleavage of the Alzheimer's amyloid precursor protein. Proc Natl Acad Sci USA 104:11062–11067. doi:10.1073/pnas.0609621104

Potolicchio I, Carven GJ, Xu X, Stipp C, Riese RJ, Stern LJ, Santambrogio L (2005) Proteomic analysis of microglia-derived exosomes: metabolic role of the aminopeptidase CD13 in neuropeptide catabolism. J Immunol 175:2237–2243

Provencher SW, Glockner J (1981) Estimation of globular protein secondary structure from circular dichroism. Biochemistry 20:33–37. doi:10.1021/bi00504a006

Prusiner SB (1998) Prions. Proc Natl Acad Sci USA 95:13363–13383. doi:10.1073/pnas.95.23.13363

Rezaei H, Eghiaian F, Perez J, Doublet B, Choiset Y, Haertle T, Grosclaude J (2005) Sequential generation of two structurally distinct ovine prion protein soluble oligomers displaying different biochemical reactivities. J Mol Biol 347:665–679

Saito T, Bunnett NW (2005) Protease-activated receptors: regulation of neuronal function. Neuromolecular Med 7:79–99. doi:10.1385/NMM:7:1-2:079

Sawaya MR, Sambashivan S, Nelson R, Ivanova MI, Sievers SA, Apostol MI, Thompson MJ, Balbirnie M, Wiltzius JJ, McFarlane HT, Madsen AO, Riekel C, Eisenberg D (2007) Atomic structures of amyloid cross-beta spines reveal varied steric zippers. Nature 447:453–457. doi:10.1038/nature05695

Shmerling D, Hegyi I, Fischer M, Blattler T, Brandner S, Gotz J, Rulicke T, Flechsig E, Cozzio A, von Mering C, Hangartner C, Aguzzi A, Weissmann C (1998) Expression of amino-terminally truncated PrP in the mouse leading to ataxia and specific cerebellar lesions. Cell 93:203–214. doi:10.1016/S0092-8674(00)81572-X

Silveira JR, Raymond GJ, Hughson AG, Race RE, Sim VL, Hayes SF, Caughey B (2005) The most infectious prion protein particles. Nature 437:257–261. doi:10.1038/nature03989

Solforosi L, Criado JR, McGavern DB, Wirz S, Sanchez-Alavez M, Sugama S, DeGiorgio LA, Volpe BT, Wiseman E, Abalos G, Masliah E, Gilden D, Oldstone MB, Conti B, Williamson RA (2004) Cross-linking cellular prion protein triggers neuronal apoptosis in vivo. Science 303:1514–1516. doi:10.1126/science.1094273

Sreerama N, Woody RW (2000) Estimation of protein secondary structure from circular dichroism spectra: comparison of CONTIN, SELCON, and CDSSTR methods with an expanded reference set. Anal Biochem 287:252–260. doi:10.1006/abio.2000.4880

Swietnicki W, Morillas M, Chen SG, Gambetti P, Surewicz WK (2000) Aggregation and fibrillization of the recombinant human prion protein huPrP90–231. Biochemistry 39:424–431. doi:10.1021/bi991967m

Tagliavini F, Forloni G, D'Ursi P, Bugiani O, Salmona M (2001) Studies on peptide fragments of prion proteins. Adv Protein Chem 57:171–201. doi:10.1016/S0065-3233(01)57022-9

Tatzelt J, Schatzl HM (2007) Molecular basis of cerebral neurodegeneration in prion diseases. FEBS J 274:606–611. doi:10.1111/j.1742-4658.2007.05633.x

Turk B, Turk D, Turk V (2000) Lysosomal cysteine proteases: more than scavengers. Biochim Biophys Acta 1477:98–111

Vella LJ, Sharples RA, Lawson VA, Masters CL, Cappai R, Hill AF (2007) Packaging of prions into exosomes is associated with a novel pathway of PrP processing. J Pathol 211:582–590. doi:10.1002/path.2145

Walsh DM, Selkoe DJ (2007) Abeta oligomers: a decade of discovery. J Neurochem 101:1172–1184. doi:10.1111/j.1471-4159.2006.04426.x

Xiang W, Windl O, Wunsch G, Dugas M, Kohlmann A, Dierkes N, Westner IM, Kretzschmar HA (2004) Identification of differentially expressed genes in scrapie-infected mouse brains by using global gene expression technology. J Virol 78:11051–11060. doi:10.1128/JVI.78.20.11051-11060.2004

Yadavalli R, Guttmann RP, Seward T, Centers AP, Williamson RA, Telling GC (2004) Calpain-dependent endoproteolytic cleavage of PrPSc modulates scrapie prion propagation. J Biol Chem 279:21948–21956. doi:10.1074/jbc.M400793200

Zhang Y, Pothakos K, Tsirka SA (2005) Extracellular proteases: biological and behavioral roles in the mammalian central nervous system. Curr Top Dev Biol 66:161–188. doi:10.1016/S0070-2153(05)66005-X